The strengthening effect caused by an elastic contrast-part II: stratification by a thin stiff layer

Dominique Leguillon, Eric Martin

The strengthening effect caused by an elastic contrast—part II: stratification by a thin stiff layer

Dominique Leguillon, **Eric Martin**

Abstract To quantify the gain in strength of a layered heterogeneous structure caused by the elastic contrast between the layers, especially if no crack deflection is observed at the interface, two original mechanisms baptized "step-over" and "jump-through" were proposed in Part I. They addressed the ability of a crack to pass through an interface and were applied to a bimaterial structure; whereas part II is dedicated to a homogeneous beam embedding a thin stiff film. The asymptotic expansions differ significantly since the small parameter is now the layer thickness. Unlike the first part where it was difficult to evidence the gain in toughness due to the superposition of two effects: a simultaneous increase in stiffness and in toughness, here it is possible to characterize the strength enhancement in using a single parameter. A discussion of the possibility to repeat the effect by multiplying the thin films is presented at the end.

Keywords Fracture mechanics · Brittle materials · Laminate structures

D. Leguillon (✉)
Institut Jean Le Rond d'Alembert, CNRS UMR 7190,
Université Pierre et Marie Curie, 4 place Jussieu,
75005 Paris, France
e-mail: dominique.leguillon@upmc.fr

E. Martin
Laboratoire des Composites Thermo-Structuraux,
CNRS UMR 5801, Université de Bordeaux,
3 rue La Boétie, 33600 Pessac, France
e-mail: martin@lcts.u-bordeaux1.fr

1 Introduction

Part I (Leguillon and Martin 2012b) provides an analysis of the role of an interface in improving the toughness of a material, especially if no crack deflection is observed. "Step-over" and "jump-through" mechanisms are applied to a bimaterial made of two layers of equal thickness, a compliant and a stiff one. For simplicity, the first is predominant if the elastic contrast between the materials is high, while the second takes over otherwise. Both avoid a paradox: it is not necessary to indefinitely increase the load for a crack to cross an interface between a compliant and a stiff material, as confirmed by intuition and testing. Our goal was to show, against conventional wisdom, that the addition of a rigid layer could improve the apparent toughness of a structure, even without deflection along the interface. However, the strengthening enhancement is not clearly evidenced due to the superimposition of two effects: the simultaneous increase in apparent stiffness and toughness.

Note that it is usually the addition of compliant slabs that is supposed to enhance the damage tolerance. But, from our point of view, this is not directly for their elastic properties but more likely for their high toughness; these slabs are able to withstand very large deformations, even in the plastic range, before breaking. On the contrary, there is a tendency to associate stiff layers with brittleness, which not exact either, there is no relationship between these two properties and all situations may be encountered.

In an attempt to extend this concept, we propose here to study the influence of the succession of thin stiff and thick soft layers on the apparent toughness of a laminate even if no crack deflection occurs. A crack in a soft layer approaching a stiffer one tends to decelerate and stop (weak singularity, Leguillon and Sanchez-Palencia 1992). Then growth can be achieved only by increasing the load, it is the origin of the toughening effect. The situation is exactly reversed for a crack in a rigid layer. The crack tends to accelerate and to pass through this layer toward the compliant layer located ahead (strong singularity). By varying the thicknesses of the soft and rigid layers, the rigid layers being somewhat sacrificed, it seems possible to improve the apparent toughness of a layered structure (Chai and Ravichandran 2007). This enhancement can be characterized by a single parameter in the present case.

Okumura and de Gennes (2001) have approached this phenomenon but have studied the limit case of a dramatically small Young's moduli contrast 0.0002 with the additional assumption that compliant layers are by far much thinner than the stiff ones, both being at some nanometers scale in nacre. Xia et al. (2012) were interested in a quite similar problem of the peeling of an adhesive tape periodically reinforced by small rigid plates. However, such 1D models simply highlight the phenomena but have sometimes the disadvantage of hiding difficulties. Besides the materials mentioned at the beginning of this presentation, there are examples in the nature which appear to meet the same idea: the succession of winter and summer wood in the growth of tree trunks (Simon 2009), the presence or absence of stratification in volcanic materials which lead to two very different types of volcanic eruptive properties for instance (Gudmundsson 2009).

The outline of this second part follows that of Part I. After analyzing a 3-point bending test (Sect. 2), two mechanisms of a crack crossing interfaces are studied: the "step-over" (Sect. 3) and the "jump-through" (Sect. 4). The penetration mechanism called He and Hutchinson is not studied here, it only served as a comparison in the previous paper (He and Hutchinson 1989). In order to avoid the coupling between the strengthening and the stiffening effects observed in Part I, the stiffer layer is here much thinner that the compliant layer. Thus, the stiffness of the specimen is not affected whereas the strength does increase as we shall try to prove. The asymptotics are now carried out with respect to the thin layer thickness (preferentially to the crack extension length or the ligament width as done in Part I). Many notations and hypothesis refer to Part I, but we tried to make this second part as self-contained as possible.

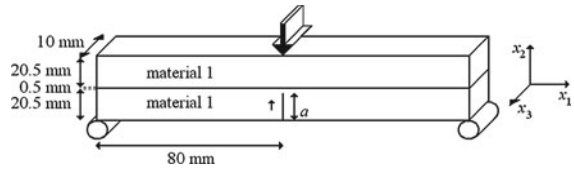

Fig. 1 The 3-point bending 10 × 41.5 × 160 mm specimen embedding a thin layer of stiff material in the middle with a crack with length a growing in the bottom layer

2 The 3-point bending test

In this second part we still consider a bimaterial but the stiffer material (material 2) appears only as a thin layer with thickness e between two substrates made of the same material 1 (Fig. 1). We assume that the surface flaws are regularly distributed and their size is negligible at our scale, which allows considering the material (and the interface) as homogeneous with appropriate fracture parameters. Moreover, the interface is assumed to be tough enough to avoid any crack deflection.

Our statement is mainly based on a thought experiment with fictitious materials; however it proves useful to consider also realistic situations. Parameters for material 1 are those of PMMA: $E^{(1)} = 3,500\,\text{MPa}$, $\nu = 0.3$, $G_{\text{Ic}}^{(1)} = 0.35\,\text{MPa mm}$ ($K_{\text{Ic}}^{(1)} = 36.7\,\text{MPa mm}^{1/2}$), $\sigma_c^{(1)} = 70\,\text{MPa}$. Material 2, the thin layer in between, is from 2 to 50 times stiffer. As an example, parameters for glass are selected: $E^{(2)} = 70,000\,\text{MPa}$, $\nu = 0.3$, $G_{\text{Ic}}^{(2)} = 0.01\,\text{MPa mm}$ ($K_{\text{Ic}}^{(2)} = 27.7\,\text{MPa mm}^{1/2}$), $\sigma_c^{(2)} = 100\,\text{MPa}$. As before, it may be noted that the choice of Poisson's ratios are not very realistic, it is a little bit more than 0.3 for PMMA and a little bit less for glass. This choice is made to focus solely on Young's modulus contrast, knowing that the role of Poisson's ratio is not critical within the range of values involved here.

Note that interesting experiments and modeling have been carried out by Chai and Ravichandran (2007) on this kind of stacking sequence (glass/epoxy instead of glass/PMMA).

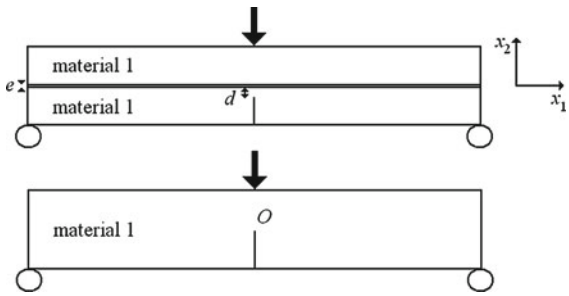

Fig. 2 The actual specimen with a thin stiff layer with thickness e between two substrates of the same material (*top*) and the limit domain ($e \to 0$) without thin layer (*bottom*)

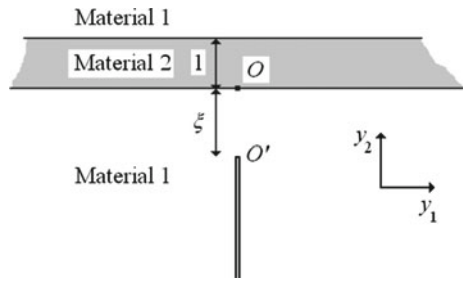

Fig. 3 The inner domain, the dimensionless width of the stretched stiff layer is 1

The ligament d is assumed to be smaller or of the same order of magnitude than e (Fig. 2, top), this assumption being as usual a posteriori checked.

There are two small parameters d and e. For practical reasons, the asymptotic expansions are carried out with respect to e, and d is a parameter. It is easier to vary the ligament width by buttoning and unbuttoning nodes than to vary the layer thickness which requires a remeshing. The outer expansion is written

$$\underline{U}^e(x_1, x_2, d) = \underline{U}^0(x_1, x_2) + \text{small correction} \qquad (1)$$

where $\underline{U}^0(x_1, x_2)$ is solution to the simplified problem of a crack in a homogeneous material (Fig. 2, bottom). No details, neither the layer thickness nor the ligament width, are visible. The behavior of $\underline{U}^0(x_1, x_2)$ is described by the classical Williams expansion

$$\underline{U}^0(x_1, x_2) = \underline{U}^0(O) + K_{\mathrm{I}}\sqrt{r}\,\underline{u}_{\mathrm{I}}(\theta) + \cdots \qquad (2)$$

Using the same notations as in Part I, K_{I} is the stress intensity factor (SIF) of the crack tip singularity and $\underline{u}_{\mathrm{I}}(\theta)$ the shape function associated to mode I, mode II is absent for symmetry reasons. The matching procedure being the same (Leguillon and Sanchez-Palencia 1987; Leguillon and Martin 2012b), but carried out with respect to e instead of d, it leads to an inner expansion of the form

$$\begin{aligned}\underline{U}^e(x_1, x_2, d) &= \underline{U}^e(ey_1, ey_2, e\xi)\\ &= \underline{U}^0(O) + K_{\mathrm{I}}\sqrt{e}\,\underline{V}_0^1(y_1, y_2, \xi) + \cdots\\ &= \underline{U}^0(O)\\ &\quad + K_{\mathrm{I}}\sqrt{e}\left(\sqrt{\rho}\,\underline{u}_{\mathrm{I}}(\theta) + \hat{\underline{V}}_0^1(y_1, y_2, \xi)\right)\\ &\quad + \cdots \quad \text{with } \xi = d/e \end{aligned} \qquad (3)$$

With (the lower index 0 means that there is no crack extension, see Sects. 3 and 4)

$$\underline{V}_0^1(y_1, y_2, \xi) = \sqrt{\rho}\,\underline{u}_{\mathrm{I}}(\theta) + \hat{\underline{V}}_0^1(y_1, y_2, \xi) \qquad (4)$$

This is a crucial point in matched asymptotics and especially with a thin layer. It is not possible to solve directly for $\underline{V}_0^1(y_1, y_2, \xi)$ in the unbounded inner domain shown in Fig. 3 because of its behaviour at infinity (it grows indefinitely like $\sqrt{\rho}$ due to the matching conditions). It is necessary to proceed by superposition [see (4)] where $\hat{\underline{V}}_0^1(y_1, y_2, \xi)$ tends to 0 at infinity. The variational formulation of the problem in this new unknown function involves integrals within the unbounded thin layer and along its interfaces. Roughly, they converge because, within the layer, the polar angle θ behaves like $1/\rho$ as $\rho \to \infty$ and thus $\hat{\underline{V}}_0^1(y_1, y_2, \xi)$ is solution to a well-posed problem.

As before (Leguillon and Martin 2012b), the actual SIF K'_{I} at the tip O' of the primary crack can be calculated

$$\underline{U}_0^e(x_1, x_2, d) = \cdots + K_{\mathrm{I}}\kappa\sqrt{r'}\,\underline{u}_{\mathrm{I}}(\theta') + \cdots \Rightarrow K'_{\mathrm{I}} = K_{\mathrm{I}}\kappa \qquad (5)$$

The coefficient κ is a function of ξ (the dimensionless ligament width) and is shown in Fig. 4 for different values of Young's moduli contrast $R = E^{(1)}/E^{(2)}$. The theoretical value 0 at $\xi = 0$ is forced, it is difficult to numerically capture it. Note that the location of the singular point is varying in the inner domain, thus it was difficult to compute κ using path independent integrals for any ξ without defining new contours at each new tip location. It was calculated by identifying the crack opening at the first node with the opening mode I, but this procedure is less accurate and tends to underestimate the actual value. This is why κ was first calculated at $\xi = 1$ by both methods (path independent integral and identification) and then a correction using a multiplier based on this first double determination was systematically applied for the other values of ξ. We checked on different meshes that this way of doing worked well.

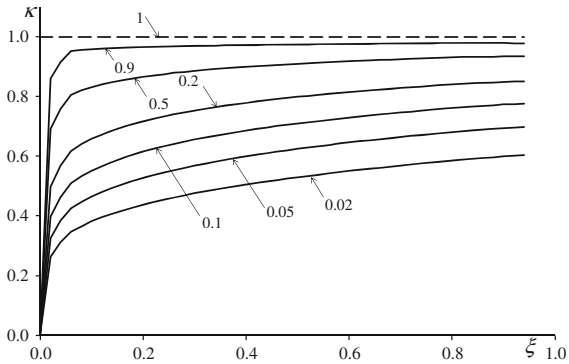

Fig. 4 The coefficient κ function of ξ for different values of Young's moduli contrast $R = 0.9, 0.5, 0.2, 0.1, 0.05, 0.02$. The *dashed line* corresponds to the homogeneous case $R = 1$

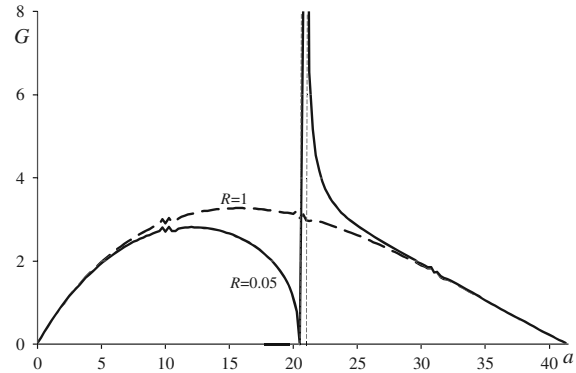

Fig. 5 The ERR G (MPa mm) function of the crack length a (mm) for two Young's moduli contrast $R = 1$ and 0.05 for a 1 mm displacement of the loading point. As before the 0 value is forced

The toughening effect can be directly expressed through the coefficient $1/\kappa$ since the primary crack is assumed to travel quasistatically in material 1

$$K_{\mathrm{I}}' = K_{\mathrm{I}c}^{(1)} \Rightarrow K_{\mathrm{I}}/K_{\mathrm{I}c}^{(1)} = 1/\kappa \text{ with } K_{\mathrm{I}c}^{(1)} = \sqrt{\frac{E^{(1)} G_{\mathrm{I}c}^{(1)}}{2\pi(1-\nu^2)}} \tag{6}$$

where $K_{\mathrm{I}c}^{(1)}$ is the critical value of the mode I SIF in material 1, it relies on $G_{\mathrm{I}c}^{(1)}$ through the Irwin relation (the unusual $1/2\pi$ coefficient is due to the normalization chosen for the William's expansion, see Part I for details). Here the comparison is easy to do because at the leading order, the structure behaves like the homogeneous material 1 [see (1)].

Figure 5 shows the energy release rate (ERR) G (the derivative of the potential energy with respect to the crack length) computed by FE, function of the total crack length a for two Young's moduli contrast $R = 1$ and 0.05 for a 1 mm displacement of the loading point. We observe the same phenomenon as in the bimaterial case (Leguillon and Martin 2012b), G decreases to 0 as the crack approaches the first interface which is the effect of a weak singularity, whereas it indefinitely grows as the crack approaches the second interface (strong singularity). However, this remains localized because of the thinness of the layer.

The ERR reduction can "slow down" a crack that is momentarily trapped near the interface with the rigid layer whereas the same crack in a homogeneous structure, at the same load level, would grow and lead to almost ruin the structure. But obviously if, after being trapped, the crack restarts, it leads also to the total failure in a quite similar manner to that occurring in a homogeneous material. The point to retain is that the crack was "delayed" (see Sect. 5 for an estimation of the gain).

Once again, in the following, the interfaces between materials 1 and 2 are assumed to be strong enough to prevent any debonding. The case of the crack propagating along its axis without branching is the only one retained. A mechanism analogous to that described below can be analyzed taking into account the crack deflection and the interface debonding instead of the penetration into material 2.

A family of simulations is conducted with the same fracture properties in the two materials: $G_{\mathrm{I}c}^{(1)} = G_{\mathrm{I}c}^{(2)}$, $\sigma_c^{(1)} = \sigma_c^{(2)}$, to highlight the gain of toughness obtained only through the contrast of Young's moduli (a kind of Einstein's thought experiment).

3 The "step-over" mechanism

In this section and in the next one we propose an extension of the mixed criterion (Leguillon 2002). It relies on an incremental energy balance and leads to the conclusion that, in most cases, the crack jump over a finite and often small length. This is completed by a stress condition which usually determines univocally the length of the jump. The role of the rigid layer can be compared to a kind of blunting (Leguillon et al. 2007) which leads to a formulation similar to the one developed herein.

The "step-over" mechanism should a priori take into account a crack starting from the first interface and

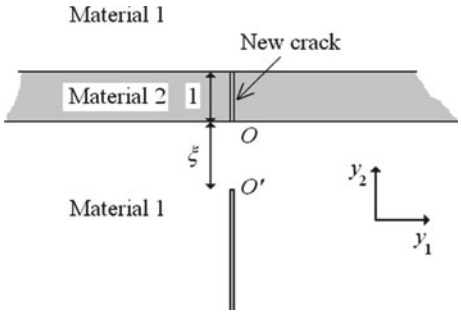

Fig. 6 The step-over mechanism observed from the inner point of view

extending forward in the thin layer and possibly in the next material 1. Nevertheless, the conditions for the crack to extend beyond the thin film and reach material 1 are not met during the nucleation phase. It must be remembered that the primary crack grows in a stable manner in the first part of material 1 and that a nucleation ahead of it in the same material is unrealistic even if enhanced by the thin layer. Anyway, this is checked numerically. Moreover, for simplicity and to retain only the situations most frequently observed numerically, we will consider only cracks which pass completely through the thin layer as shown in Fig. 6.

The inner expansion can be written now

$$\begin{aligned}\underline{U}_1^e(x_1, x_2, d) &= \underline{U}_1^e(ey_1, ey_2, e\xi)\\ &= \underline{U}^0(O) + K_{\mathrm{I}}\sqrt{e}\underline{V}_1^1(y_1, y_2, \xi) + \cdots\end{aligned} \tag{7}$$

The lower index 1 corresponds to a problem settled on the inner domain with a crack extension in material 2 (Fig. 6) as opposed to the index 0 in Sect. 2.

The energy balance leads to (δW^p is the change in potential energy prior to and following the new crack onset and t the specimen thickness)

$$\delta W^p = K_{\mathrm{I}}^2 e\,(A_1(\xi) - A_0(\xi))\,t \geq G_{\mathrm{Ic}}^{(2)} et \tag{8}$$

where the two coefficients $A_j(\xi)\, j = 0{,}1$ are scaling coefficients derived from $\underline{V}_j^1(y_1, y_2, \xi)$ computed in the inner domains respectively defined by Figs. 3 and 6 (i.e. without and with a crack extension). On the right hand side, et is the newly created crack surface. On the other side, t is a consequence of the plane elasticity assumption and e comes from the asymptotic expansions (3) and (7). Then the energy condition can be written

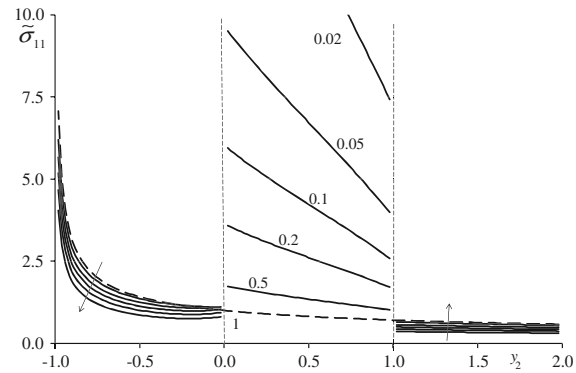

Fig. 7 The dimensionless function $\tilde{\sigma}_{11}(0, y_2, 1)$ for different Young's moduli contrast: $R = 0.5$, 0.2, 0.1, 0.05 and 0.02 following the *arrows*. The *dashed line* is the homogeneous case $R = 1$, the very weak contrast $R = 0.9$ is not plotted because the two curves almost merge. The crack tip singularity is visible on the left and the discontinuities due to the interfaces are visible at $y_2 = 0$ and $y_2 = 1$

$$K_{\mathrm{I}}^2\,(A_1(\xi) - A_0(\xi)) \geq G_{\mathrm{Ic}}^{(2)} \tag{9}$$

Using the same notations as in Part I, the stress condition gives

$$\begin{aligned}&\frac{K_{\mathrm{I}}}{\sqrt{e}}\tilde{\sigma}_{11}(0, y_2, \xi) \geq \sigma_c^{(2)} \quad \text{for } 0 < y_2 \leq 1\\ &\quad\Rightarrow \frac{K_{\mathrm{I}}}{\sqrt{e}}\tilde{\sigma}_{11}(0, 1_-, \xi) \geq \sigma_c^{(2)}\end{aligned} \tag{10}$$

with

$$\underline{\tilde{\sigma}}(y_1, y_2, \xi) = \mathbf{C} : \nabla_y^{\mathrm{S}}\underline{V}^1(y_1, y_2, \xi) \tag{11}$$

where $\mathbf{C}$ is the elastic tensor and ∇_y^S the symmetric part of the gradient operator with respect to the space variables y_i. The notation 1_- in (10) holds for the limit as $y_2 \leq 1$ and $y_2 \to 1$. The function $\tilde{\sigma}_{11}(0, y_2, 1)$ (i.e. for $\xi = 1$, the ligament dimensionless width equals the layer thickness) is shown in Fig. 7; it is piecewise decreasing which justifies (10).

Taking into account (6) leads to two conditions on the unknown parameter ξ

$$\begin{cases}\left(\frac{K_{\mathrm{Ic}}^{(1)}}{\kappa(\xi)}\right)^2 (A_1(\xi) - A_0(\xi)) - G_{\mathrm{Ic}}^{(2)} \geq 0\\ \frac{K_{\mathrm{Ic}}^{(1)}}{\kappa(\xi)\sqrt{e}} - \frac{\sigma_c^{(2)}}{\tilde{\sigma}_{11}(0,1_-,\xi)} \geq 0\end{cases} \tag{12}$$

The smallest ξ corresponding to the highest remote load must be retained to simultaneously fulfill the two conditions (see Sect. 5). Results are shown in Table 1 for different elastic contrasts R and three different layer thicknesses $e = 0.5$, 0.1 and 0.02 mm.

Table 1 The dimensionless ligament width ξ for various elastic contrasts: $R = 0.5, 0.2, 0.1, 0.05$ and 0.02 and for three different layer thicknesses: $e = 0.02$, 0.1 and 0.5 mm; $\xi < 0.04$ means it is below the accuracy due to the mesh refinement. Here $\sigma_c^{(2)} = 70$ MPa($\sigma_c^{(1)}$ plays no role) and $G_{Ic}^{(1)} = G_{Ic}^{(2)} = 0.35$ MPa mm

R	0.5	0.2	0.1	0.05	0.02
ξ for $e = 0.02$ mm	<0.04	0.22	0.72	2.07	6.96
ξ for $e = 0.1$ mm	<0.04	0.22	0.72	2.07	6.96
ξ for $e = 0.5$ mm	<0.04	<0.04	0.72	2.07	6.96

Unlike Part I, the crack extension length l is no longer an adjustable parameter ($l = e$) and the two conditions (12) do not merge, the criterion remains two-fold. Moreover, it is noteworthy that the energy condition $(12)_1$ does not depend on the layer thickness e. Thus, for e small enough, the mechanism is governed by the energy condition as seen in Table 1, most of the results being independent of e. Note that $\xi \leq 0.1$ means $e \geq 10d$, in this case results obtained in the bimaterial case of Part I are taking over. But the crucial point is that the mechanism is very difficult or even impossible to trigger when the elastic contrast is low.

The nucleation phase predicts the onset of a crack through the thin stiff layer but emphasis is put again on the fact that this is not a final state. Once the thin layer is broken, there are 3 crack tips, the primary crack tip opening is enhanced by the onset of a crack ahead of it and the primary crack starts to grow forward again. The two tips of the new crack undergo a strong singularity (Leguillon and Sanchez-Palencia 1992; Leguillon et al. 2000; Leguillon and Martin 2012a) and moves respectively forward for the front tip and backward for the other. These combined effects tend to reduce and then eliminate the ligament.

4 The "jump-through" mechanism

The analogous to the "jump-through" mechanism described in Part I is shown in Fig. 8. This mechanism should a priori take into account a crack starting from the primary tip O' (Fig. 3) and extending forward through the ligament (material 1), then in the thin layer (material 2) and possibly in the next substrate (material 1 again). Moreover, as before, the conditions for the crack to extend beyond the thin film and reach material 1 are not met during the nucleation phase. Finally, for simplicity, we will consider only cracks which pass completely through the ligament and the thin layer but

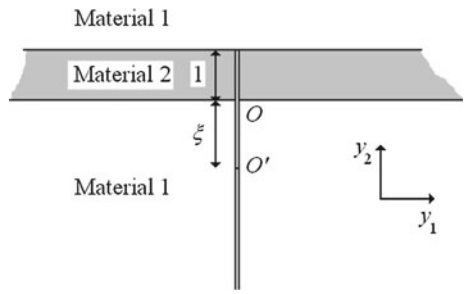

Fig. 8 The "jump-through" mechanism observed from the inner point of view

do not penetrate the next substrate shown in Fig. 8. It has been numerically observed that, during the nucleation phase, the crack rarely partly breaks the thin layer.

The crack jump is made of the broken ligament (width d) and the broken layer (width e). The total length of the crack extension is $l = d + e$. The two inner expansions (3) and (7) still hold but now the index 1 in (7) corresponds to Fig. 8.

As above, the energy balance leads to

$$\delta W^p = K_I^2 e \left(A_1(\xi) - A_0(\xi)\right) t \geq G_{Ic}^{(1)} dt + G_{Ic}^{(2)} et \tag{13}$$

where $A_1(\xi)$ now derives from $\underline{V}_1^1(y_1, y_2, \xi)$ computed in the inner domain defined by Fig. 8. The surface of the new crack splits in two parts dt in material 1 and et in the layer, they occur in the right hand side member. The left handside is unchanged in its form. Then

$$K_I^2 \left(A_1(\xi) - A_0(\xi)\right) \geq \xi G_{Ic}^{(1)} + G_{Ic}^{(2)} \tag{14}$$

There are now two stress conditions, one in material 1 and the other in material 2

$$\begin{cases} \frac{K_I}{\sqrt{e}} \tilde{\sigma}_{11}(0, y_2, \xi) \geq \sigma_c^{(1)} \text{ if } y_2 < 0 \Rightarrow \frac{K_I}{\sqrt{e}} \tilde{\sigma}_{11}(0, 0_-, \xi) \geq \sigma_c^{(1)} \\ \frac{K_I}{\sqrt{e}} \tilde{\sigma}_{11}(0, y_2, \xi) \geq \sigma_c^{(2)} \text{ if } 0 < y_2 \leq 1 \Rightarrow \frac{K_I}{\sqrt{e}} \tilde{\sigma}_{11}(0, 1_-, \xi) \geq \sigma_c^{(2)} \end{cases} \tag{15}$$

Since $\tilde{\sigma}_{11}(0, y_2, \xi)$ is a stepwise decreasing function of y_2 (i.e. separately decreasing in the different domains

but discontinuous at the interfaces, Fig. 7). The notation 0_ holds for the limit as $y_2 \leq 0$ and $y_2 \to 0$ and 1_ for the limit as $y_2 \leq 1$ and $y_2 \to 1$.

The two conditions (15) can be resumed in

$$K_{\mathrm{I}} \geq \Sigma_c(\xi)\sqrt{e} \text{ with } \Sigma_c(\xi) = \mathrm{Max}\left[\frac{\sigma_c^{(1)}}{\tilde{\sigma}_{11}(0,0_-,\xi)}; \frac{\sigma_c^{(2)}}{\tilde{\sigma}_{11}(0,1_-,\xi)}\right] \quad (16)$$

In addition, since it is assumed that prior to the jump, the primary crack was growing in material 1 in a stable manner, then according to (6), (14) and (16) provide two inequalities

$$\begin{cases} \left(\frac{K_{\mathrm{Ic}}^{(1)}}{\kappa(\xi)}\right)^2 (A_1(\xi) - A_0(\xi)) - \xi G_{\mathrm{Ic}}^{(1)} - G_{\mathrm{Ic}}^{(2)} \geq 0 \\ \frac{K_{\mathrm{Ic}}^{(1)}}{\kappa(\xi)\sqrt{e}} - \Sigma_c(\xi) \geq 0 \end{cases} \quad (17)$$

The first one relies on the energy balance whereas the second one does on the stress condition and depends on e. As above in Sect. 3 the smallest ξ corresponding to the highest remote load must be retained to simultaneously fulfill the two conditions. Table 2 shows the dimensionless ligament width ξ for various elastic contrast R and for 3 different layer thicknesses: $e = 0.02$, 0.1, 0.5 mm and the same conclusions can be drawn concerning the role of e and the accuracy.

Table 3 summarizes Tables 1 and 2 results stating which mechanism seems preferentially activated when the fracture properties are the same in the layer and the substrates, for different elastic contrasts and various layer thicknesses. It provides also the gain in toughness $g = 1/\kappa(\xi_c)$ (Eq. 5) where ξ_c is fixed by Table 1 or 2 according to the activated mechanism. Table 3 and parameter g are the most significant results of this work.

In the homogeneous case, the load at failure is 0.112 kN (Part I), it corresponds to the row $R = 1$. For various elastic contrasts and layer thicknesses this critical load varies according to the coefficient g (Table 3). The "jump-through" is favored by low contrast and small thicknesses and evolves in "step-over" when the contrast increases (i.e. R decreases). For a given thickness, it seems that the "jump-through" leads to an improvement in toughness, the gain increases when the contrast increases, whereas the opposite occurs for the "step-over".

In the particular case of a thin layer of glass ($e = 0.5$ mm) inserted in a PMMA specimen, the promoted mechanism is the step over, the gain $g = 18\%$ lead to a failure load 0.132 kN (instead of 0.112 kN for the homogeneous specimen). It is important to note that although the glass is by far much more brittle than PMMA, the high contrast of Young's moduli ($R = 20$) still leads to an increase in the failure load of the specimen and thus an apparent improvement in toughness.

Table 2 The dimensionless ligament width ξ for various elastic contrasts: $R = 0.5$, 0.2, 0.1, 0.05 and 0.02 and for three different layer thicknesses: $e = 0.02$, 0.1, 0.5 mm. Here $\sigma_c^{(1)} = \sigma_c^{(2)} = 70$ MPa and $G_{\mathrm{Ic}}^{(1)} = G_{\mathrm{Ic}}^{(2)} = 0.35$ MPa mm

R	0.5	0.2	0.1	0.05	0.02
ξ for $e = 0.02$ mm	2.87	3.26	3.4	3.55	3.88
ξ for $e = 0.1$ mm	0.08	0.72	0.74	0.76	0.76
ξ for $e = 0.5$ mm	<0.04	<0.04	0.14	0.14	0.14

Table 3 The mechanisms preferentially activated for $\sigma_c^{(1)} = \sigma_c^{(2)} = 70$ MPa and $G_{\mathrm{Ic}}^{(1)} = G_{\mathrm{Ic}}^{(2)} = 0.35$ MPa mm and the gain in toughness $g = (1/\kappa) - 1$ (%)

R	1	0.5	0.2	0.1	0.05	0.02
$e = 0.02$ mm		Jump-through	Jump-through	Jump-through	Jump-through	Step-over
g (%)	0	3	8	13	21	23
$e = 0.1$ mm		Bimaterial Case	Jump-through	Jump-through /step-over	Step-over	Step-over
g (%)	0		20	33	29	23
$e = 0.5$ mm		Bimaterial case	Bimaterial case	Step-over	Step-over	Step-over
g (%)	0			34	29	23

5 Miscellanous comments on the numerical simulations

In both cases, "step-over" and "jump-through" mechanisms, the twofold criterion was solved by retaining the smallest of the two values of ξ given by each condition before originating the crack growth; it is the only way to satisfy both criteria simultaneously. The curves below give a numerical justification of this argument. Figure 9 (bottom) shows the stress condition for 3 different layer thicknesses $e = 0.5$, 0.1 and 0.02 mm for the "step-over" and $R = 0.1$, whereas Fig. 9 (top) shows the energy condition which is independent of e. Units on the vertical axes are useless. In this case, as already observed, it is the energy condition that governs the inequality system and ξ keeps constant whatever e. It may be noted, however, that for $e = 0.5$ mm the two conditions give similar solutions (the energy condition gives $\xi = 0.72$ and the stress one $\xi = 0.76$).

Figure 10 shows the same in the case of "jump-through". The situation is now different: it is the stress

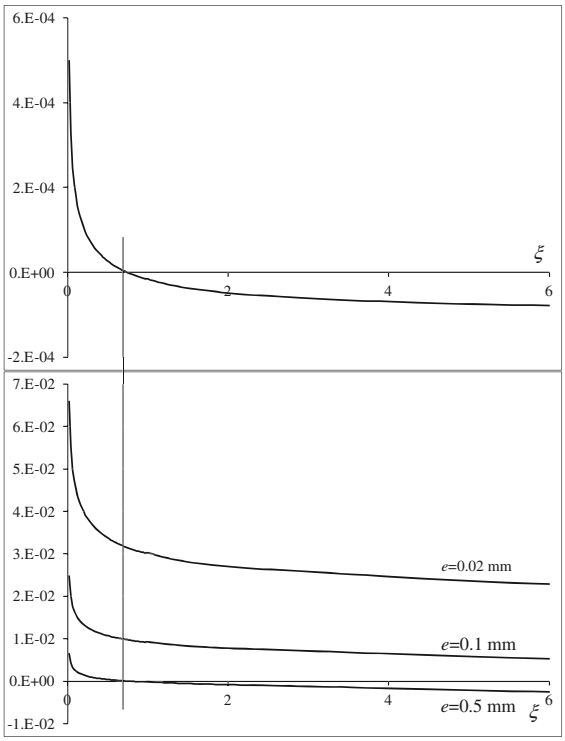

Fig. 9 The stress condition (*bottom*) for 3 different layer thicknesses and the energy condition (*top*) for the "step-over" mechanism and $G_{\mathrm{Ic}}^{(1)} = G_{\mathrm{Ic}}^{(2)}$, $\sigma_c^{(1)} = \sigma_c^{(2)}$

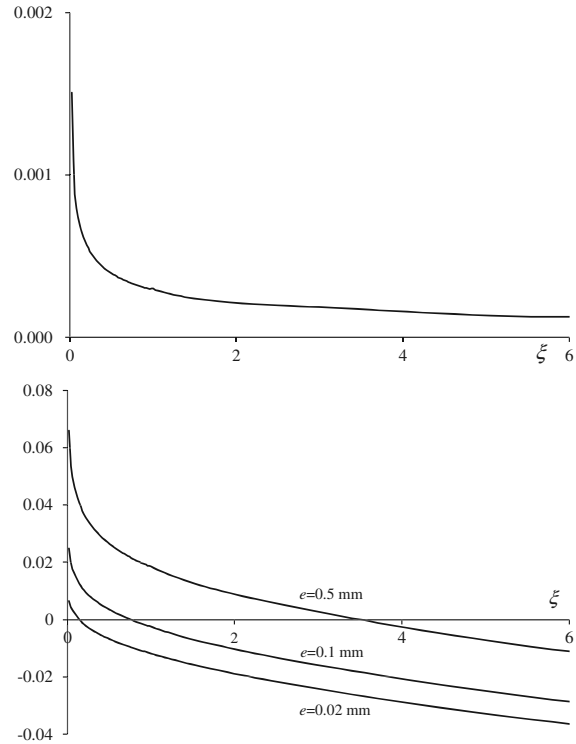

Fig. 10 The stress condition (*bottom*) for 3 different layer thicknesses and the energy condition (*top*) for the "step-over" mechanism and $G_{\mathrm{Ic}}^{(1)} = G_{\mathrm{Ic}}^{(2)}$, $\sigma_c^{(1)} = \sigma_c^{(2)}$

condition that governs the mechanism. Moreover (16) and then $(17)_2$ are discontinuous and it is the first item of (16) which is dominant with the present parameters, i.e. the condition at $y_2 = 0_-$. This is not always the case and at lower elastic contrasts R, it is the second item of (16) that prevails at least as the ligament is small.

6 Discussion

As stated in the introduction, it could be expected to repeat the strengthening effect exhibited in Fig. 5 by multiplying the interfaces. Quick calculations were performed in the situation described in Fig. 11, i.e. that of a $10 \times 41.5 \times 160$ mm specimen made of a compliant material and embedding three thin layers (3×0.5 mm) of a stiff material ($R = 0.05$).

The analogue of Fig. 5 is shown in Fig. 12. For a primary crack larger than 2.5 mm and smaller than 5 mm, the strengthening effect of the first interface plays its role, the crack is trapped in material 1 by the first stiff

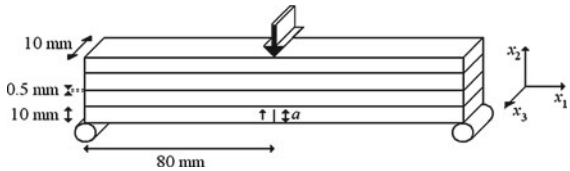

Fig. 11 The 3-point bending multi-layer 10 × 41.5 × 160 mm specimen with a crack growing in the bottom layer

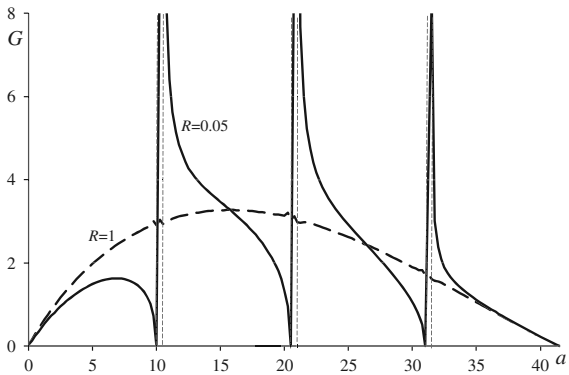

Fig. 12 The ERR G (MPa mm) (*solid line*) function of the crack length a (mm) for $R = 1$ and 0.05 for a 1 mm displacement of the loading point of the multi-layer specimen. Note that 0 values are forced for better clarity

layer. But, if the load sufficiently increases, one of the mechanisms of crack jump described in Sects. 3 and 4 initiates and the crack penetrates the stiffer layer, then it is clear from Fig. 12 that if a substantial part of the excess energy is fed back into rupture (Leguillon and Martin 2012b), nothing will stop the crack until the complete ruin of the specimen.

On the other hand, if the excess energy is entirely dissipated by various mechanisms such as acoustic waves, the crack will be trapped ahead of each rigid layer provided that the distance at which it stops ($G = G_{Ic}$) is larger than the calculated length in (17). The condition for this to hold true is essentially based on the geometry of the specimen and the chosen test which lead to a global decrease of G once the middle line is passed. It is visible in the homogeneous case (dashed line in Fig. 12) and affects also the heterogeneous one. Here in Fig. 12, the third layer seems to be the only one likely to stop the crack, but anyway the extra load leading to the final ruin remains small because it adds to the already increased load to cross the first interface.

7 Conclusion

A crack crossing an interface is not a simple mechanism and cannot be solved by using the Griffith criterion and the classical tools of brittle fracture mechanics. Thanks to the coupled criterion (Leguillon 2002), we propose two mechanisms called "step-over" and "jump-through" which respond to the paradox: it is not necessary to indefinitely increase the load for a crack to cross an interface between a compliant and a stiff material, as confirmed by intuition and testing. Thus the gain in toughness brought by stratification of a material is not "infinite" but still substantial. Of course, it would be very interesting to compare this model with experiments, unfortunately there are very few of these tests in the literature. We plan to develop ourselves experiments in the future.

Obviously, it would be necessary to conduct also further simulations by varying the number of layers, varying the elastic contrast R between the layers and changing the ratio of the compliant and stiff layers thicknesses. Decreasing the contrast is expected to store less energy but at the same time reduces the strengthening effect according to Fig. 4. On the other hand, increasing the thickness of compliant layers is expected to absorb a part of the excess energy. All these changes could be incorporated in a future optimization process.

References

Chai H, Ravichandran G (2007) Transverse fracture in multilayers from tension and line-wedge indentations. Int J Fract 145:299–312

Gudmundsson A (2009) Deflection of dykes into sills at discontinuities and magma-chamber formation. Tectonophysics 500(1–4):50–64

He MY, Hutchinson JW (1989) Crack deflection at an interface between dissimilar elastic materials. Int J Solids Struct 25:1053–1067

Leguillon D (2002) Strength or toughness? A criterion for crack onset at a notch. Eur J Mech A Solids 21:61–72

Leguillon D, Lacroix C, Martin E (2000) Matrix crack deflection at an interface between a stiff matrix and a soft inclusion. C R Acad Sci Paris (série IIb) 328:19–24

Leguillon D, Quesada D, Putot C, Martin E (2007) Size effects for crack initiation at blunt notches or cavities. Eng. Fract. Mech. 74:2420–2436

Leguillon D, Martin E (2012a, to appear) Crack nucleation at stress concentration points in composite materials—application to the crack deflection by an interface. In: Mantic V (ed) Mathematical methods and models in composites. Computational and experimental methods in structures. Imperial College Press, London

Leguillon D, Martin E (2012b, in preparation) The strengthening effect caused by an elastic contrast—part I: the bimaterial case

Leguillon D, Sanchez-Palencia E (1987) Computation of singular solutions in elliptic problems and elasticity. Wiley, New York

Leguillon D, Sanchez-Palencia E (1992) Fracture in heterogeneous materials, weak and strong singularities. In: Ladevèze P, Zienkiewicz O (eds). Proceedings of the European conference on new advances in computational structural mechanics. Elsevier, Amsterdam, pp 229–236

Okumura K, de Gennes P-G (2001) Why is nacre strong? Elastic theory and fracture mechanics for biocomposites with stratified structures. Eur Phys J E4:121–127

Simon P (2009) Approche multi-échelle du comportement mécanique du bois dans le plan transverse. PhD thesis, INSA Lyon, Villeurbanne

Xia S, Ponson L, Ravichandran G, Bhattacharya K (2012, to appear) Toughening and asymmetry in peeling of heterogeneous adhesives. Phys Rev Letter